CHEMISTRY OF MATERIALS

Subscriber access provided by Columbia Univ Libraries

Article

Conjugated Sidechain Isolated Donor-Acceptor Copolymers based on Benzo[1,2-b:4,5-b']dithiophene-alt-dithienylbenzotriazole: Synthesis and Photovoltaic Properties

Jie Min, Zhi-guo Zhang, Siyuan Zhang, and Yongfang Li

Chem. Mater., **Just Accepted Manuscript** • DOI: 10.1021/cm3017006 • Publication Date (Web): 30 Jul 2012

Downloaded from http://pubs.acs.org on July 31, 2012

Just Accepted

"Just Accepted" manuscripts have been peer-reviewed and accepted for publication. They are posted online prior to technical editing, formatting for publication and author proofing. The American Chemical Society provides "Just Accepted" as a free service to the research community to expedite the dissemination of scientific material as soon as possible after acceptance. "Just Accepted" manuscripts appear in full in PDF format accompanied by an HTML abstract. "Just Accepted" manuscripts have been fully peer reviewed, but should not be considered the official version of record. They are accessible to all readers and citable by the Digital Object Identifier (DOI®). "Just Accepted" is an optional service offered to authors. Therefore, the "Just Accepted" Web site may not include all articles that will be published in the journal. After a manuscript is technically edited and formatted, it will be removed from the "Just Accepted" Web site and published as an ASAP article. Note that technical editing may introduce minor changes to the manuscript text and/or graphics which could affect content, and all legal disclaimers and ethical guidelines that apply to the journal pertain. ACS cannot be held responsible for errors or consequences arising from the use of information contained in these "Just Accepted" manuscripts.

ACS Publications
High quality. High impact.

Chemistry of Materials is published by the American Chemical Society. 1155 Sixteenth Street N.W., Washington, DC 20036

Published by American Chemical Society. Copyright © American Chemical Society. However, no copyright claim is made to original U.S. Government works, or works produced by employees of any Commonwealth realm Crown government in the course of their duties.

Conjugated Sidechain Isolated D-A Copolymers Based on Benzo[1,2-b:4,5-b']dithiophene-alt-dithienylbenzotriazole: Synthesis and Photovoltaic Properties

Jie Min, Zhi-Guo Zhang*, Siyuan Zhang, and Yongfang Li*

Beijing National Laboratory for Molecular Sciences, CAS Key Laboratory of Organic Solids, Institute of Chemistry, Chinese Academy of Sciences, Beijing 100190 (China)
E-mail: liyf@iccas.ac.cn (Y. Li), zgzhangwhu@iccas.ac.cn (Z. Zhang)

Abstract

Conjugated sidechain isolated D-A copolymers, based on the donor unit of benzodithiophene (BDT) with thiophene conjugated side chain, thiophene pi-bridge and the acceptor unit of benzotriazole (BTA) with or without fluorine substitution (PBDT-FBTA and PBDT-HBTA), were designed and synthesized for elucidating their structure–property relationships. The copolymer films demonstrated well defined absorption peaks with steep absorption edges, consistent with their rigid and ordered structures in the solid films. The substitution of thiophene conjugated side chain on the BDT unit in the copolymers aroused 15 nm red-shifted absorption in comparison with its polymer analogues with alkoxy side chains on BDT unit. Compared to **PBDT-HBTA**, **PBDT-FBTA** with two fluorine atoms substitution on BTA unit demonstrated lower HOMO energy level, higher hole mobility and significantly better photovoltaic performance. The PSC based on **PBDT-FBTA/** $PC_{70}BM$ (1:2, w/w) with 5% DIO additive displayed a power conversion efficiency of 6.0% with a J_{sc} of 11.9 mA/cm^2, a V_{OC} of 0.75 V and a FF of 67.2%, under the illumination of AM1.5G, 100 mW/cm^2. Even at a thicker active layer of 400 nm, the PSC still demonstrated a higher PCE of 4.74%. The results indicate that **PBDT-FBTA** is a promising polymer donor material for future application of large area PSCs.

Keywords: polymer solar cells, two-dimension-conjugated polymers, side chain isolation, D−A copolymers

1. Introduction

Bulk heterojunction (BHJ) polymer solar cells (PSCs)[1] based on *p*−type conjugated polymers as donor[2-9] and *n*−type fullerene derivatives[10] as acceptor have been intensively studied in recent years for the generation of affordable, clean, and renewable energy. Advantages of the BHJ PSCs include low−cost fabrication of large−area devices, light weight, mechanical flexibility, and easy tunability of chemical properties of the photovoltaic materials.

It has been realized that an ideal polymer donor in PSCs should exhibit broad absorption with high absorption coefficient in the visible region, high hole mobility, suitable electronic energy levels matching to the fullerene acceptor, and appropriate compatibility with fullerene acceptor to form nanoscale bicontinuous network.[2-9] These specific design criteria can offer high values of short circuit current (J_{sc}), open circuit voltage (V_{oc}) and fill factor (FF) of the PSCs, which are related to the power conversion efficiency (PCE) of the PSCs by the following equation: PCE = $(J_{sc} \times V_{oc} \times \mathrm{FF})/P_{in}$, where P_{in} is the input light power.

For broadening the absorption, the two-dimension-conjugated (2-D-conjugated) polymers with conjugated side chain (see Type 1 in **Figure** 1) were designed and synthesized in our group.[11] The 2-D-conjugated polymers possess higher hole mobility thanks to the 2-D-conjugated structure, and broader absorption deriving from both the main chains and conjugated side chains. Thus this family of 2-D-conjugated polythiophenes demonstrated good device performances in PSCs[11a] and organic field−effect transistors (OFETs).[12] Now this strategy has been successfully extended to develp high efficiency polymers. Copolymers (PBDTTT) of benzodithiophene (BDT) and thieno[3,4−b]−thiophene (TT) is one of the most efficient photovoltaic materials in the PSCs[6]. Huo et. al successfully applied the 2-D conjugation concept to PBDTTT structure by thienyl-substitution on the BDT unit. [5b] The 2-D conjugated polymer exhibit better thermal stabilities, red-shifted absorption spectra, lower HOMO levels, significantly higher hole mobility, and greatly improved photovoltaic properties, in comparison with the corresponding alkoxy substituted copolymers. [5b]

To overcome the steric hindrance induced by the large conjugated side chain and improve the planarity and optical properties, we recently proposed a "side-chain-isolation" concept and developed the 2-D-conjugated polythiophenes with unsubstituted thienyl spacer (Type 2 in **Figure 1**).[13] In such polymers, due to the proper side chain distance and the improved planarity of polymer backbone, these polymers demonstrated red−shifted and enhanced absorption thus improved photovoltaic properties. Considering the diverse molecular engineering approach under this side chain isolated photovoltaic materials, such as changing the nature of side chain and spacer as well as introducing donor−acceptor (D−A) concept in the conjugated side chain,[14-16] the side chain isolated photovoltaic materials could open a new way for developing high performance polymer solar cells.

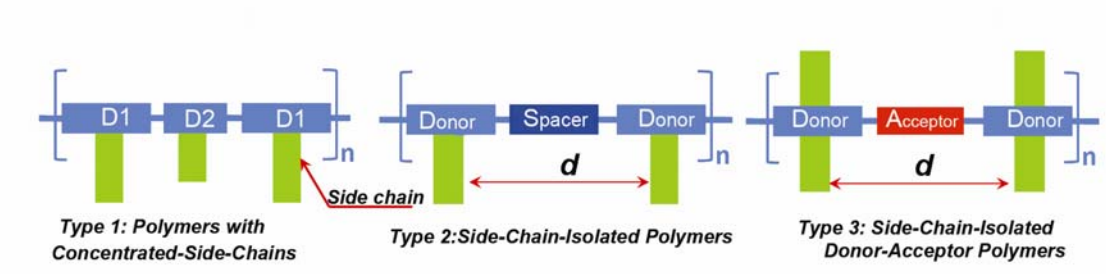

Figure 1. Three typical molecular architectures of 2-D-conjugated polymers. (Here *d* represents the distance between the conjugated side chains, and the alkyl chain group attached on the acceptor unit was omitted for clarity due to its negligible effect on the planarity.)

To further extend the absorption and modulate the energy levels, here we introduce D−A concept by changing the side chain isolation spacer partly with the acceptor unit of benzotriazole (BTA) [17] or fluorinated BTA,[18] and synthesized two new 2-D-conjugated and side-chain-isolated D−A copolymers (Type 3 in **Figure 1**) of PBDT-HBTA and PBDT-FBTA (see **Scheme 1**). The incorporation of Fluorine atom in the two-dimension architecture is inspired by its unique features as demonstrated by You *et al.*, such as strong inter- and intramolecular interactions and smallest electron-withdrawing group in size.[18-19] In the copolymers, the benzodithiophene (BDT) unit with thiophene conjugated side chain[20] was used as donor unit to form the 2-D-conjugated polymers, in considering the good planarity and symmetric structure of BDT unit and the high photovoltaic efficiency of the copolymers based on the thiophene-substituted BDT unit.[5a,20,21] The 2-D-conjugated and sidechain-isolated D−A copolymers combine the advantages of broader absorption and higher hole mobility of the 2-D-conjugation, less steric hindrance of the sidechain-isolation, and the broad absorption and lower HOMO energy level of the D-A copolymerization. As a result, the two dimensional character is clearly demonstrated in the as-developed polymers. For example, in comparison with the linear copolymer analogues with alkoxy side chains on BDT unit[17a] and that with alkyl side chain on BDT unit,[18] the absorption spectra with thiophene conjugated side chain is red-shifted by ca. 15 nm. Among these two copolymers, the fluorinated copolymer **PBDT−FBTA** demonstrated promising photovoltaic properties. The PSC based on **PBDT−FBTA** as donor and $PC_{70}BM$ as acceptor showed a power conversion efficiency of 6.0% with an open circuit voltage of 0.75 V, under the illumination of AM1.5G, 100 mW/cm^2.

2. Results and Discussion

2.1. Synthesis of Monomers and Polymers

The synthetic routes of fluorinated dithienylbenzotriazole (FBTA) and the D-A copolymers are respectively depicted in Schemes 1 and 2. The fluorine atom substituted dithienylbenzotriazole was firstly described by You *et al* but with low yield[18]. Here an easier synthesis procedure with higher overall yield was explored in detail. The reduction of 4,5-difluoro-2-nitroaniline with tin powder in 12 N HCl gave 4,5-difluoro-1,2-phenylenediamine (1), which was treated with $NaNO_2$ to afford compound 2. Alkylation of compound 2 was carried out in methanol with potassium tert-butoxide and 1-bromooctane in a good yield. The position of the alkyl group in compound 3 was confirmed by ^1H NMR. The bromination of benzotriazole (3) was finished firstly by activation of the benzotriazole ring with trimethylsilyl group and subsequently electrophilic substitution with bromine. The fluorinated dithienylbenzotriazole (FTBA) was obtained by a stille coupling followed by an N-bromosuccinimide (NBS) bromination.

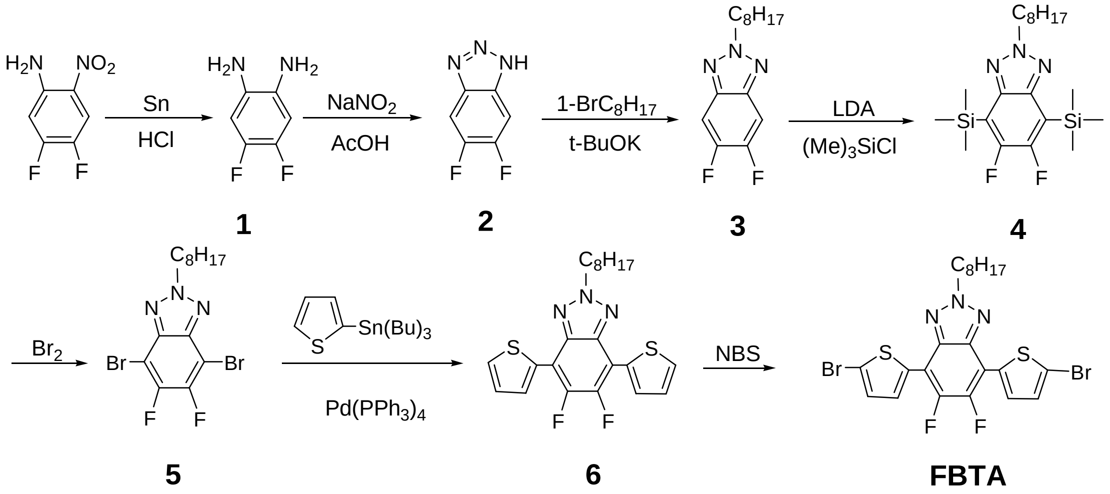

Scheme 1. Synthetic route of the fluorinated monomer (FBTA)

PBDT-HBTA and PBDT-FBTA were synthesized by Stille coupling reaction,[6] as shown in Scheme 2. The two copolymers are soluble in chlorinated solvents, such as chloroform, chlorobenzene and dichlorobenzene. The number-average molecular weight (M_n) of the polymers is 31.2K for PBDT-HBTA and 114.5K for PBDT-FBTA, with polydispersity index (PDI) of 2.60 and 2.77 respectively. Thermal stability of the polymers was investigated with thermogravimetric analysis (TGA) as shown in Figure S1 in Supporting Information (SI). The onset temperatures with 5% weight-loss (T_d) of PBDT-HBTA and PBDT-FBTA are 327 °C and 364 °C, respectively. This indicates that the copolymers are stable enough for the applications in optoelectronic devices. The data of molecular weight and T_d of the two copolymers were listed in Table 1 for a clear comparison. DSC thermogram of PBDT-FBTA (see Figure S2 in SI) shows a small endothermic peak at 110 °C, while there are no endothermic or exothermic peaks in the DSC thermogram of PBDT-HBTA in the temperature range of 30~300$^\mathrm{o}$C. The results indicate there could be some morphology transformation at ca. 110 °C for PBDT-FBTA with fluorine atoms substitution.

Table 1. Molecular weights, thermal properties and physicochemical properties of the copolymers.

Polymers	M_n (g/mol)	PDI (M_w/M_n)	T_d ^{a} (°C)	λ $_\mathrm{edg}$ $^\mathrm{b}$ (nm)	E_g ^{opt} (eV)	HOMO (eV)	LUMO (eV)	Mobility ($\mathrm{cm^2 \cdot V^{-1} s^{-1}}$)
PBDT-HBTA	81.3K	2.60	327	659	1.88	-5.13	-3.16	1.8×10^{-3}
PBDT-FBTA	317.1K	2.77	364	649	1.91	-5.26	-3.08	2.4×10^{-3}

[a] 5% weight loss temperature measured by TGA under N_2.

[b] For the polymer films.

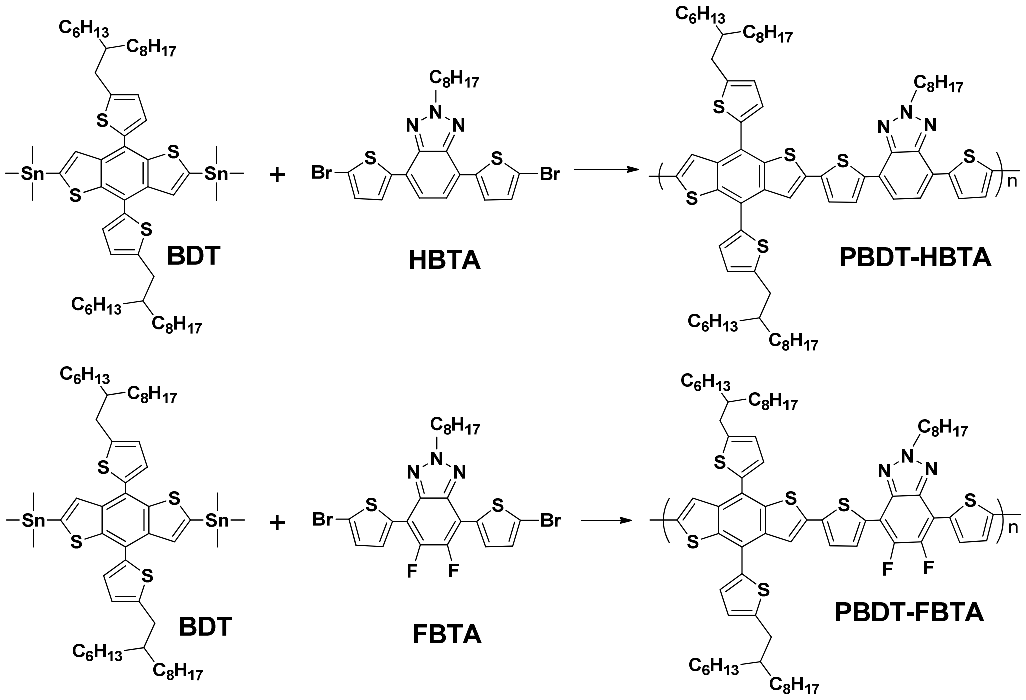

Scheme 2. Synthetic routes to the side chain isolated D-A copolymers.

2.2. Optical and Electrochemical Properties.

Figure 2 shows the absorption spectra of the polymer solutions in chloroform and films on quartz plate, and the absorption data were also listed in Table 1 for comparison. The solution and film absorptions of the two copolymers display similar absorption band with well defined peaks and steep absorption edges. In comparison with the analogue copolymer with alkoxy side chains on BDT unit[17a] and that with alkyl side chain on BDT unit[18], the absorption spectrum of **PBDT-HBTA** with thiophene conjugated side chain is red-shifted by ca. 15 nm. The absorption edges of the polymer films are at 659 nm for **PBDT−HBTA** and 649 nm for **PBDT−FBTA**, corresponding to optical bandgaps of 1.88 eV and 1.91 eV, respectively. Moreover, the two copolymer films show well−defined absorption spectra, indicating the ordered polymer chains and densely packed side chains in the polymer film, which should be beneficial to higher hole mobility and photovoltaic performance. The absorption of **PBDT−FBTA** film is only red-shifted a little than that of its solution, which reveals strong aggregation existed in the solution for the fluorinated polymer.[19] When the polymer solutions were heated to 80 °C, the absorption peaks blue shifted in some extent, as shown in **Figure 2a and 2b**, and the shoulder peak at ca. 600 nm weakened, implying partial dis-aggregation of the polymer backbone at the high temperature.

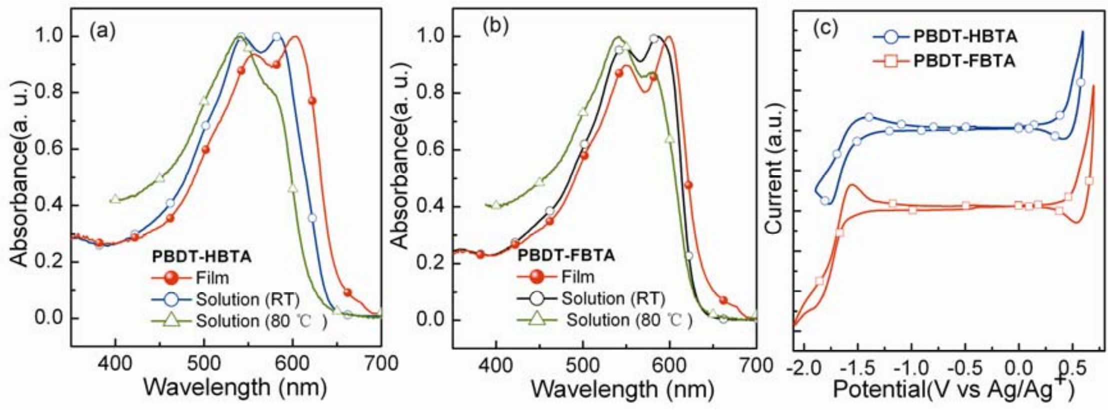

Figure 2. The dichlorobenzene solution and film absorption spectra of (a) **PDTS-HBTA** and (b) **PDTS-FBTA**. (c) Cyclic voltammograms of the polymer films on glassy carbon electrode in a 0.1 mol/L *n*−Bu_4NPF_6 acetonitrile solution at a sweep rate of 100 mV/s.

2.3. X-ray Diffraction and Hole Mobility.

The X-ray diffraction patterns of the two polymers, as shown in Figure S3 in SI, display a (100) diffraction peak at ca. 2θ = 3.70°, corresponding to an interchain *d*–spacing of 23.68 Å. This value is greater than that of P3HT (16.4 Å)[22] due to the bulky side chain on the polymers. The (010) diffraction peaks with broad feature located at ca. 2θ = 24.8°, corresponding to a facial π-π stacking distance of 3.67 Å. These results indicate that the substitution of the hydrogen with fluorine on the benzotriazole group has no effect on the interchain *d*–spacing and π-π stacking distance. While, the difference in their solid structure is revealed by their second order or third order diffraction peaks, which is properly related to the inter- and intramolecular interactions through C-F···H and F···S interactions. The crystalline characteristics of these two polymers appeared to be favorable for charge transport in PSCs.

To measure the hole mobilities of the polymers, organic field-effect transistors were fabricated in a top contact geometry using Au as the source and drain electrode. Figure S5 and Figure S6 in SI show the output and transfer curves of the OTFT devices based on **PBDT-HBTA** and **PBDT-FBTA** respectively. The calculated hole mobilities were 1.8×10^{-3} cm^2/Vs for **PBDT–HBTA** and 2.4×10^{-3} cm^2/Vs for **PBDT–FBTA** (see Table 1), confirming the relatively higher hole mobility of these two copolymers.

2.4. Electrochemical Properties

The highest occupied molecular orbital (HOMO) and the lowest unoccupied molecular orbital (LUMO) energy levels of the copolymers were measured by electrochemical cyclic voltammetry, and were calculated from the onset oxidation potential (φ_{ox}) and onset reduction potential (φ_{red}) obtained from the cyclic voltammograms of the polymers according to the following equations[23]: $E_{HOMO} = -e(\varphi_{ox}+4.71)$ (eV) and $E_{LUMO} = -e(\varphi_{red}+4.71)$, where the unit of potential is V *vs*. Ag/Ag^+. **Figure 2c** shows the cyclic voltammograms of the two polymers. The φ_{ox} and φ_{red} of **PBDT-HBTA** are 0.42 V and −1.55 V *vs*. Ag/Ag^+ respectively, corresponding to HOMO level of −5.13 eV and LUMO level of −3.16 eV. After introducing fluorine atom in **PBDT-FBTA**, its HOMO energy level is down–shifted to −5.26 eV. The HOMO and LUMO energy levels of the polymers were also shown in Table 1. The lower HOMO energy levels of **PBDT-FBTA** can provide better air stability in ambient condition and higher open circuit voltage (V_{oc}) of the PSCs with **PBDT-FBTA** as donor materials, because the V_{oc} is usually proportional to the difference between the LUMO level of the acceptor and the HOMO level of the donor.

2.5. Photovoltaic Properties.

Polymer solar cells were fabricated from **PBDT-HBTA** or **PBDT-FBTA** as donor and (6,6)-phenyl-C_{70}-butyric acid methyl ester ($PC_{70}BM$) as acceptor with a general device structure (see the inset of **Figure 3**) of ITO/PEDOT:PSS/Polymer:$PC_{70}BM$/Ca(20 nm)/Al(90 nm). The active layers were spin-coated from chlorobenzene (CB) solution of the donor and acceptor, 1,8-diiodooctane (DIO) was used as processing additive to optimize the morphology, and pre-thermal annealing at 110 °C for 10 min was performed before deposition of the metal top electrode.

Table 2. The comparison of the photovoltaic properties of the PSCs based on polymer/$PC_{70}BM$ (1:1, w/w) without or with DIO additive under the illumination of AM1.5G, 100 mW/cm^2.

Polymers	DIO	V_{oc} (V)	J_{sc} (mAcm^{-2})	FF (%)	PCE (%)	Thickness (nm)
PBDT−HBTA	No	0.60	5.38	52.8	1.70	80 nm
	Yes	0.58	7.41	56.5	2.43	110 nm
PBDT−FBTA	No	0.72	5.68	57.2	2.34	80 nm
	Yes	0.73	7.61	62.1	3.45	86 nn
	Yes	0.76	10.94	53.8	4.47	202 nm

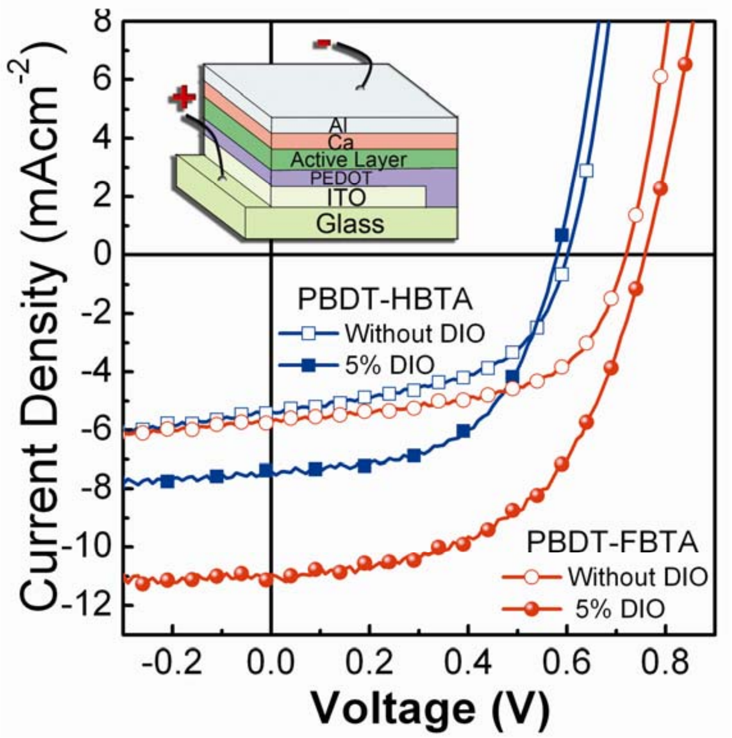

Figure 3. Current density−voltage curves of the PSCs based on polymer/PC$_{70}$BM (1:1, w/w) with and without DIO as a processing additive, under the illumination of AM1.5G, 100 mW/cm^2. The inset shows the schematic diagram of the device.

Figure 3 shows the *J-V* curves of the PSCs based on the copolymer/PC$_{70}$BM (1:1, w/w) with and without DIO processing additive, under the illumination of AM1.5G, 100 mW/cm^2, and the photovoltaic parameters of the devices are summarized in **Table 2**. In the absence of the additive, the PSC devices based on polymer/PC$_{70}$BM (1:1, w/w) exhibit relatively poor performance with a PCE of only 1.53% for **PDBT-HBTA** and 2.34% for **PDBT-FBTA**. The fluorinated polymer **PDBT-FBTA** exhibited a V_{OC} of 0.73 V, 0.1 V higher than that of **PDBT-HBTA**, which is benefitted from its lower-lying HOMO energy level. The higher hole mobility of **PDBT-FBTA** is expected to contribute in part to the higher photocurrents, higher fill factors and better device performance. The addition of 5% DIO to the blend solution dramatically improved the photovoltaic performance of the devices. As shown in the *J*−*V* curves of the PSCs based on polymer/$PC_{70}BM$ (1:1, w/w) with DIO additive, both polymers show improved efficiency than that without the additive, due mainly to significantly increased currents. The device based on **PBDT-FBDA**/$PC_{70}BM$ (1:1, w/w) with 5% DIO additive demonstrated a PCE of 4.47% with a high J_{SC} of 10.96 mA/cm^2, a high V_{OC} of 0.76 V and a FF of 53.8%.

Table 3. The effect of the active layer thickness on the photovoltaic performance of the PSCs based on a PDTS-FBTA/$PC_{70}BM$ (1: 2, w/w) with DIO additive, under the illumination of AM1.5G, 100 mW/cm^2.

Active Layer Thickness (nm)	V_{oc} (V)	J_{sc} (mAcm^{-2})	FF (%)	PCE (%)
400 nm	0.75	10.82	58.4	4.74
190 nm	0.75	11.90	67.2	6.00
102 nm	0.77	10.03	71.6	5.53

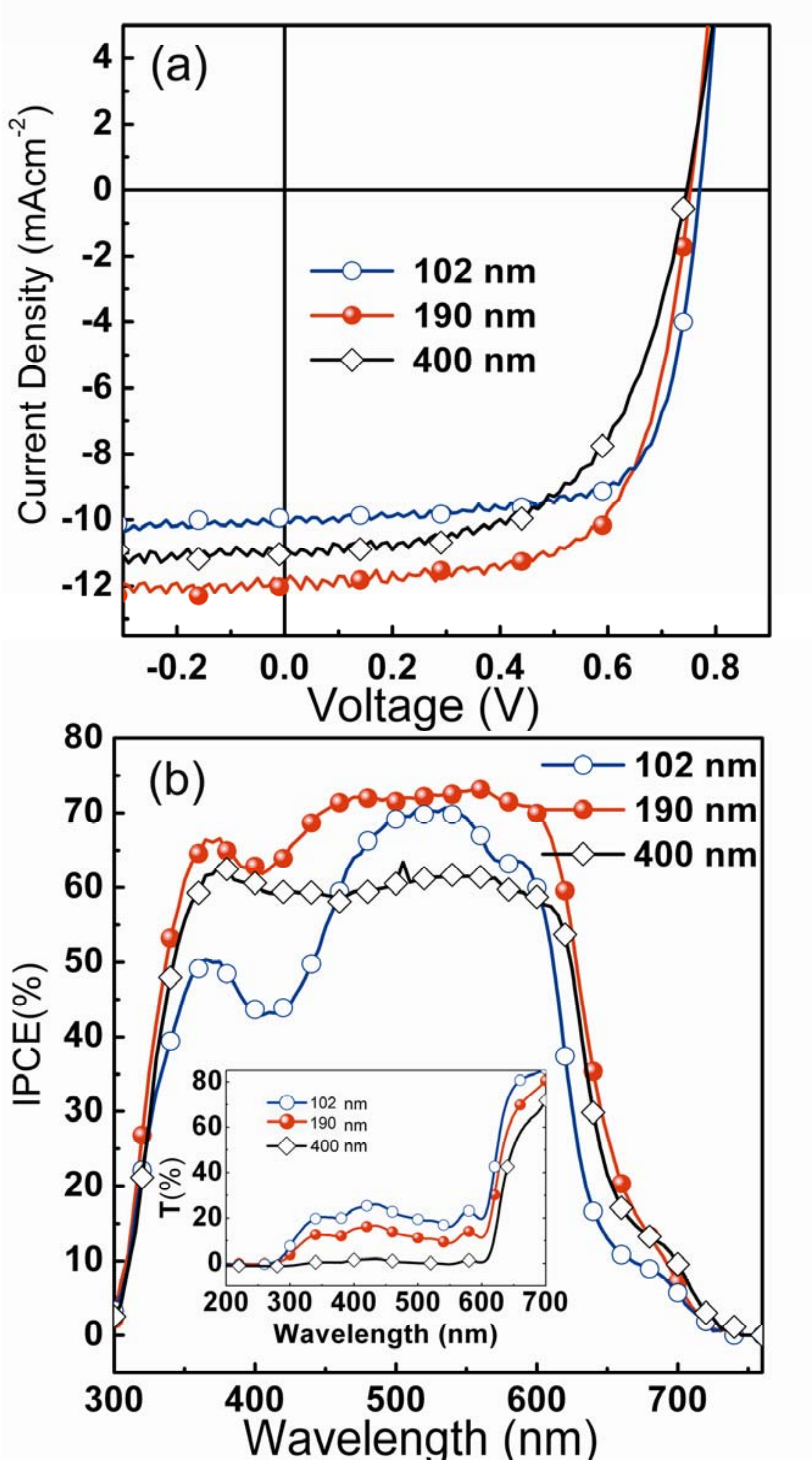

Figure 4. (a) Current density−voltage curves of the PSCs based on **PBDT-FBTA**/PC$_{70}$BM (1:2, w/w) with DIO as additive and with different active layer thickness, under the illumination of AM1.5G, 100 mW/cm^2; (b) Incident-photon-to-converted−current efficiency (IPCE) spectra of the PSCs based on **PBDT-FBTA**/PC$_{70}$BM (1:2, w/w) blend film with DIO as additive. The inset of **Figure 4b** shows transmission spectrum of the active layer.

Considering the promising photovoltaic properties of the fluorinated polymer **PBDT-FBTA**, device optimization was further performed by changing the weight ratios of **PBDT-FBTA** donor and $PC_{70}BM$ acceptor and the thickness of the active layers. The optimized weight ratio of **PBDT-FBTA**: $PC_{70}BM$ is 1:2. **Figure 4(a)** shows the J-V curves of the PSCs based on **PBDT-FBTA**/$PC_{70}BM$ (1:2, w/w) with DIO processing additive and with different active layer thickness, under the illumination of AM1.5G, 100 mW/cm^2, and the photovoltaic parameters of the devices are summarized in **Table 3**. The IPCE and transmission spectra based on the various blends are shown in Figure 4b. From the transmission spectrum of the active layer (see the inset of **Figure 4b**), we can see that thicker active layer can ensure better light-harvesting ability, and ca. 90% light was absorbed in the wavelength range of 300-620 nm for the film at 190 nm. At an active layer thickness of 102 nm, a PCE of 5.53% was obtained together with a notable FF of 71.6% and a J_{SC} of 10.03 mA/cm^2. The FF of 71.6% is the highest value in the PSCs with the 2-D-conjugated polymers as donor, which indicates that the charge flow in the device is well-balanced and no significant recombination loss occurs within the active layer under this condition. Under an optimal active layer thickness of 190 nm, the device exhibits a high J_{sc} of 11.90 mA cm^{-2} with a broad and high IPCE over 70% in the wavelength range of 450-630 nm (see **Figure 4(b)**). Together with a V_{OC} of 0.75 V and a fill factor of 67.2%, a further improved PCE of 6.0% was achieved. Interestingly, even at a thicker active layer of 400 nm, the PSC still demonstrated a higher PCE of 4.74%. The insensitivity of the photovoltaic performance of the PSCs on the active layer thickness should be benefitted from the higher hole mobility of the polymer, and it is of crucial importance for large area fabrication of the device in future commercial applications.

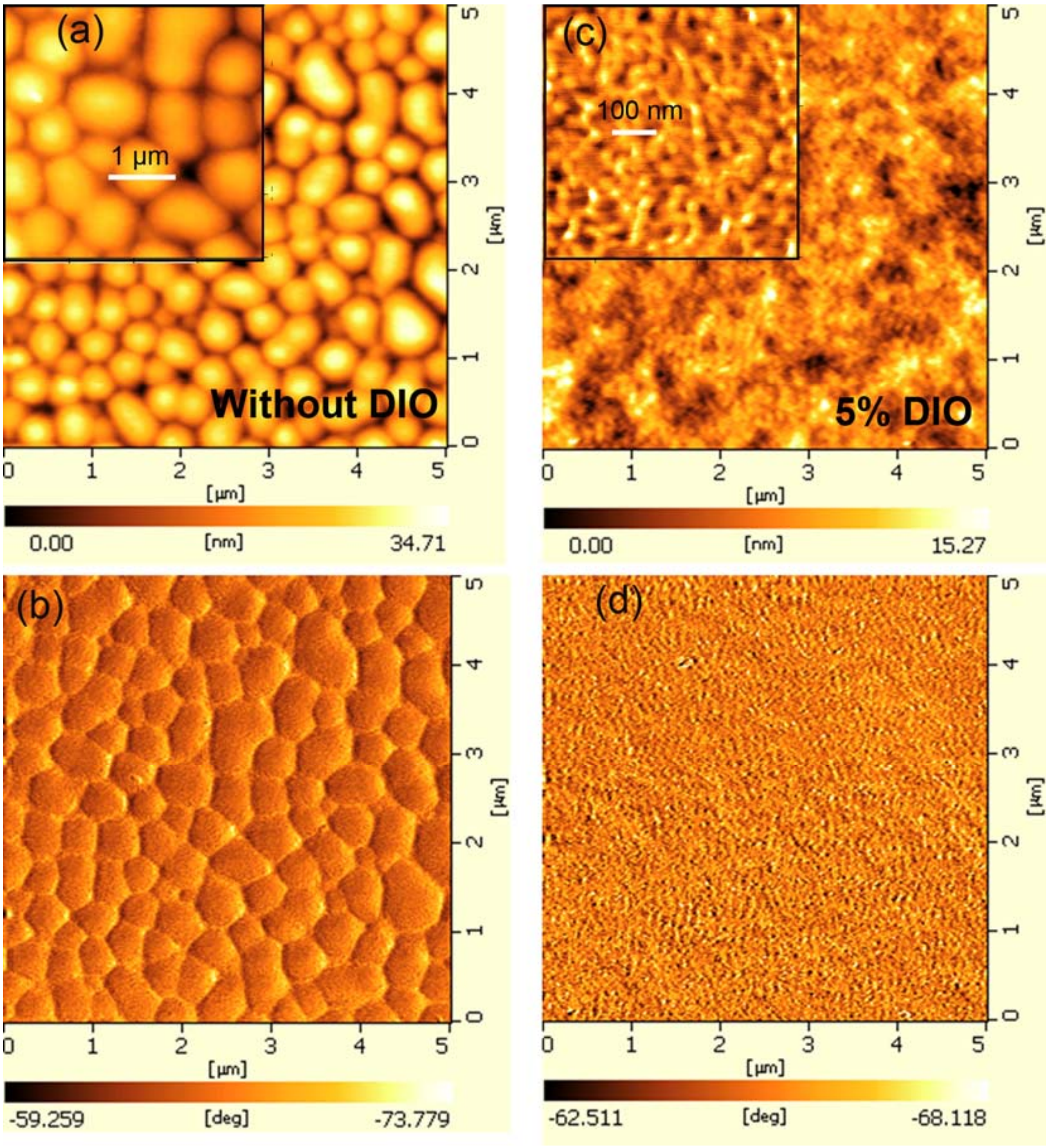

Figure 5. Tapping mode AFM (a) topography image and (b) phase image of the blend film of **PBDT-FBTA**/PC$_{70}$BM (1: 2, w/w) without DIO; (c) topography image and (d) phase image of the blend film of **PBDT-FBTA**/PC$_{70}$BM (1: 2, w/w) with DIO.

The effect of DIO additive is most clearly visualized from atomic force microscopy (AFM) images of **PBDT-FBTA**/PC$_{70}$BM (1: 2, w/w) blend film with or without DIO additive, as shown in **Figure 5**. Without DIO, the composite film exhibits micro-scale phase separation, suggesting poor dispersion of $PC_{70}BM$ in the polymer matrix (**Figure 5a** and **5b**). In contrast, nano–morphology with 20–30 nm domain size is clearly visible for the film with 5% DIO additive. The bicontinuous network with nano–scale phase separation improved the exciton dissociation and carrier collection efficiency, thus leading to an increase in short-circuit current density as well as the device efficiency. The GIXRD measurement of the polymer/PCBM blend film with and without DIO can provide further evidence on the change of the blend film structures (see Figure S4 in SI). For the blend film, the decreased peak intensity of the blend film with 5% DIO, compared to blend film without DIO, indicates the crystalline domain size within the film is decreased. This result is consistent with the morphology change.

3. Conclusions

In conclusion, we synthesized two new 2-D-conjugated and side-chain-isolated D-A copolymers, **PBDT-HBTA** and **PBDT-FBTA**, based on thiophene-substituted BDT donor unit, BTA acceptor unit without or with fluorine substitution, and thiophene π-bridges between the donor and acceptor units, for the studies on the relationship of molecular structure and photovoltaic properties of the polymer photovoltaic materials. The copolymer films demonstrated well defined absorption peaks with steep absorption edges, consistent with their rigid and ordered structures in the solid films. The substitution of thiophene conjugated side chain on the BDT unit in the copolymers aroused 15 nm red-shifted absorption in comparison with its polymer analogues with alkoxy side chains on BDT unit. Compared to **PBDT-HBTA**, **PBDT-FBTA** with two fluorine atoms substitution on BTA unit demonstrated lower HOMO energy level, higher hole mobility and significantly better photovoltaic performance. The PSC based on **PBDT-FBTA/** $PC_{70}BM$ (1:2, w/w) with 5% DIO additive displayed a power conversion efficiency of 6.0% with a J_{sc} of 11.9 mA/cm^2, a V_{OC} of 0.75 V and a FF of 67.2%, under the illumination of AM1.5G, 100 mW/cm^2. Even at a thicker active layer of 400 nm, the PSC still demonstrated a higher PCE of 4.74%. The results indicate that **PBDT-FBTA** is a promising polymer donor material for future application of large area PSCs.

4. Experimental Section

Instrumentation. ^{1}H NMR spectra were measured on a Bruker DMX–400 spectrometer with *d*–chloroform as the solvent and trimethylsilane as the internal reference. UV−visible absorption spectra were measured on a Hitachi U–3010 UV−vis spectrophotometer. Mass spectra were recorded on a Shimadzu spectrometer. Elemental analyses were carried out on a flash EA 1112 elemental analyzer. Thermogravimetric analysis (TGA) was conducted on a Perkin–Elmer TGA–7 thermogravimetric analyzer at a heating rate of 20 °C/min and under a nitrogen flow rate of 100 mL/min. Molecular weight of the polymer was measured by Gel permeation chromatography (GPC), using polystyrene as standard and THF as the eluent. The electrochemical cyclic voltammetry was performed on a Zahner IM6e Electrochemical Workstation, in an acetonitrile solution of 0.1 mol/L n-Bu_4NPF_6 at a potential scan rate of 100 mV/s with an Ag/Ag^+ reference electrode and a platinum wire counter electrode. The film morphology was measured using an atomic force microscope (AFM, SPA-400) using the tapping mode. X-ray diffraction patterns of the pristine polymer thin films were measured using a Rigaku D/ MAX 2500V/ PC diffractometer operated in grazing incidence mode.

Materails: All chemicals and reagents were purchased from commercial sources and used without further purification.

4,5-difluorobenzene-1,2-diamine (1): 4,5-difluoro-2-nitroaniline (10 g, 38 mmol) and 12 M HCl (311 mL) were put into a two-neck flask under the protection of Argon atmosphere. After cooling the mixture to 0 °C, Then tin power (33 g) was added slowly, while the reaction temperature was maintained at 25-30 °C. Continue to reaction when the tin power completely depleted after one hour at the same temperature, and then put it in the refrigerator overnight. The reaction mixture was put into 500 mL water, and then use 4 M NaOH to adjust the pH value to pH10. Meanwhile, the reaction mixture was extracted three times with ethyl acetate. The organic layer was washed with water, dried ($MgSO_4$) and then concentrated under reduced pressure. The crude product was recrystallized with methanol to obtain 4,5-difluorobenzene-1,2-diamine with a 80% yield. ^{1}H NMR (400 MHz, $CDCl_3$, ppm): 7.94 (t, 2H), 4.57 (m, 4H). Ms, m/z (%): 144. Calculated for $C_6H_6N_2F_2$: C, 50.00; H, 4.17; N, 19.44; found: C, 50.09; H, 4.12; N, 19.23.

5,6-difluoro-1H-benzo[d][1,2,3]triazole (2): Compound **1** (14 g, 0.1 mol) was dissolved in AcOH (12 ml, 0.2 mol) and 500 ml of water on heating. The reaction mixture was cooled, and a solution of $NaNO_2$ (8 g, 0.11 mol) in 200 ml of water was added at 5 °C. The reaction mixture became immediately dark-green, and it was stirred at room temperature for 1 h. The precipitate obtained after cooling was filtered off, dried in air and recrystallised from water. Yield, 81%; ^{1}H NMR (400 MHz, $CDCl_3$, ppm): 15.81 (s, 1H), 7.89 (t, 2H). Ms, m/z (%): 155. Calculated for $C_6H_3N_3F_2$: C, 46.45; H, 1.93; N, 27.10; found: C, 46.73; H, 1.92; N, 27.03.

2-(2-octyl)-5,6-difluoro-2H-benzo[d][1,2,3]triazole (3): Compound **2** (12 g, 80 mmol), potassium tert-butoxide (30 g, 200 mmol) and 1-bromooctane (29 g, 150 mmol) were dissolved in methanol (200 mL). The reaction mixture was refluxed for 24 h and monitored by TLC. The reaction mixture was then poured into saturated NH_4Cl solution, and extracted with $CHCl_3$ and washed with water twice. The organic extraction was dried over anhydrous $MgSO_4$ and the solvent was evaporated under reduced pressure. Column chromatography on silica gel was performed to obtain 4,5-difluoro-2-octylbenzotriazole as a colorless oil with a 45% yield. ^1H NMR (400 MHz, $CDCl_3$, ppm): 7.91 (t, 2H), 4.67 (d, 2H), 2.21 (m, 2H), 1.52-1.18 (m, 10H), 0.89 (t, 3H). Ms, m/z (%): 267. Calculated for $C_{14}H_{19}N_3F_2$: C, 62.92; H, 7.12; N, 15.73; found: C, 62.98; H, 7.11; N, 15.65.

4,7-di(trimethylsilyl)-2-(2-octyl)-5,6-difluoro-2H-benzo[d][1,2,3]triazole (4): 2.0 M Lithium diisopropylamide (LDA) (33 mL, 66 mmol) was added dropwise over 10 min to a solution of compound **3** (8 g, 30 mmol) and dry THF (100 mL) under argon at -78 °C. The solution was stirred for 30 min, and then trimethylsilyl chloride (7.6 g, 70 mmol) was added dropwise over 10 minutes at -78 °C. The temperature was maintained while reaction was stirred for 3h, and then the reaction was quenched with 10 mL of saturated NH_4Cl. The reaction was warmed to room temperature and poured into saturated NH_4Cl. The mixture was extracted with $CHCl_3$, washed with water twice. The organic extraction was dried over anhydrous $MgSO_4$ and the solvent was evaporated under reduced pressure. Column chromatography on silica gel was performed to obtain 4,7-di(trimethylsilyl)-5,6-difluoro-2-octylbenzotriazole as a colorless oil with a 75% yield. ^1H NMR (400 MHz, $CDCl_3$, ppm): 4.63 (d, 2H), 2.19 (m, 2H), 1.52-1.18 (m, 10H), 0.28-0.35 (t, 21H). Ms, m/z (%): 411. Calculated for $C_{14}H_{30}N_3F_2Si_2$: C, 40.87; H, 7.30; N, 10.22; found: C, 40.98; H, 7.21; N, 10.09.

4,7-dibromo-2-(2-octyl)-5,6-difluoro-2H-benzo[d][1,2,3]triazole (5): Monomer 4 (8.22 g, 20 mmol) was dissolved into $CHCl_3$ (100 mL), and bromine (9.5 g, 60 mmol) was added in one portion, and the reaction was stirred for 24 h at 60 °C, shielded from light. After cooling the mixture to room temperature, a NaOH aqueous solution was added and the aqueous layer was extracted with $CHCl_3$. The organic layer was dried over anhydrous $MgSO_4$ and the solvent was evaporated under reduced pressure. Compound **5** was obtained as a light yellow oil by column chromatography in a 85% yield. ^{1}H NMR (400 MHz, $CDCl_3$, ppm): 4.66 (d, 2H), 2.27 (m, 2H), 1.48-1.13 (m, 10H), 0.87 (t, 3H). Ms, m/z (%): 425. Calculated for $C_{14}H_{17}N_3F_2Br_2$: C, 39.53; H, 4.00; N, 9.88; found: C, 39.98; H, 4.11; N, 9.67.

2-(2-octyl)-5,6-difluoro-4,7-di(thiophen-2-yl)-2H-benzo[d][1,2,3]triazole (6): Monomer **5** (6.8 g, 16 mmol), tributyl(2-thienyl)tin (18.7 g, 50 mmol), and $Pd(PPh_3)_4$ (416 mg, 0.36 mmol) were dissolved in 150 mL of dry THF. The reaction mixture was then heated to reflux, and stirred for 48 h under a nitrogen atmosphere. After cooling, the reaction solution was extracted three times with ethyl acetate. The organic layer was washed with water, dried over anhydrous $MgSO_4$, and then concentrated under reduced pressure. Further purification was performed using silica gel column chromatography (petroleum ether/methylene = 4:1 as eluent), yellow-green crystals was obtained. The yield was 90%. ^{1}H NMR (400 MHz, $CDCl_3$, ppm): 8.23 (d, 2H), 7.51 (d, 2H), 7.23 (m, 2H), 4.76 (d, 2H), 2.57 (m, 2H), 1.58-1.18 (m, 10H), 0.91 (t, 3H). Ms, m/z (%): 433. Calculated for $C_{22}H_{23}N_3F_2S_2$: C, 60.97; H, 5.31; N, 9.70; found: C, 70.01; H, 5.37; N, 9.58.

4,7-bis(5-bromothiophen-2-yl)-2-(2-butyloctyl)-5,6-difluoro-2H-benzo[d][1,2,3]triazole (FBTA): Under the darkness, compound **6** (2.6 g, 6 mmol) was dissolved in the mixture of $CHCl_3$ (60 mL) and acetic acid (60 mL). After cooling the mixture to 0 °C, NBS (2.35 g, 13.2 mmol) was added in portions. After 12 h, the reaction mixture was extracted with $CHCl_3$ and washed by water twice and dried ($MgSO_4$). The organic solvent was evaporated. The crude product was purified by column chromatography on silica gel using 10:1 petroleum ether: methylene chloride as the eluent. Yellow crystals were obtained with 72% yield. ^1H NMR (400 MHz, $CDCl_3$, ppm): 7.93 (d, 2H), 7.15 (m, 2H), 4.71 (d, 2H), 2.33 (m, 2H), 1.44-1.12 (m, 10H), 0.88 (t, 3H). Ms, m/z (%): 591. Calculated for $C_{22}H_{21}N_3F_2S_2Br_2$: C, 44.67; H, 3.55; N, 7.11; found: C, 44.77; H, 3.47; N, 7.08.

Synthesis of PBDT-HBTA. Under the protection of Argon atmosphere, 0.5 mmol of the 2,6-Bis(trimethyltin)-4,8-bis(5-(2-ethylhexyl)thiophen-2-yl)benzo[1,2-b:4,5-b’] dithiophene (monomer BDT) [24] was put into a two-neck flask. Then 12 ml of degassed toluene and 0.5 mmol of 2-octyl-4,7-di(5-bromo-thiophen-2-yl)-2H-benzo[1,2,3] triazole (monomer HBTA)[17a] were added to the mixture. The solution was flushed with argon for 10 min, and then 25 mg of $Pd(PPh_3)_4$ was added. After another flushing with argon for 20 min, the reactant was heated to reflux for 12 h. Then the reactant was cooled to room temperature and the polymer was precipitated by adding 200 ml of methanol, filtered through a Soxhlet thimble, and then subjected to Soxhlet extraction with methanol, hexane, and chloroform. The polymer was recovered as solid from the chloroform fraction by rotary evaporation. The solid was dried under vacuum for 12 h. The yield of the polymerization reaction was about 47%. GPC: M_w = 81.3 kg/mol, M_n= 31.2 kg/mol, M_w/M_n = 2.60. ^1H NMR (400 MHz, $CDCl_3$), δ(ppm): 7.39 (m, 2H), 7.19 (m, 2H), 2.76 (m, 4H), 1.72-1.20(m, 50H), 0.79-0.90 (m, 21H).

Synthesis of PBDT-FBTA. The polymerization process was the same as that for **PBDT-HBTA**, except that monomer FBTA[18] was used instead of monomer HBTA and the reactant was refluxed for 12h. Yield: 63%. GPC: M_w = 43.0 kg/mol, M_n= 32.0 kg/mol, M_w/M_n = 1.35. ^1H

NMR (400 MHz, $CDCl_3$), δ (ppm) : 7.53-7.32 (m, 2H), 4.19 (m, 2H), 2.93 (m, 4H), 1.52-1.25(m, 50H), 0.79-0.95 (m, 21H).

Fabrication and Characterization of PSCs**:** The PSCs were fabricated with a configuration of ITO/PEDOT:PSS (40 nm)/active layer/ Ca(20 nm)/Al(90 nm). A thin layer of PEDOT:PSS (poly−(3,4−ethylenedioxythiophene): poly(styrene sulfonate)) was spin−cast on pre−cleaned ITO−coated glass from a PEDOT:PSS aqueous solution (Baytron P VP AI 4083 from H. C. Starck) at 2000 rpm and dried subsequently at 150 °C for 30 min in air, then the device was transferred to a glove box, where the active layer of the blend of the polymer and fullerene derivative was spin−coated onto the PEDOT:PSS layer. Finally, a Ca/Al metal top electrode was deposited in vacuum onto the active layer at a pressure of ca. 5×10^{-5} Pa. The active area of the device was 4 mm^2. The thickness of the active layer was determined by an Ambios Tech. XP−2 profilometer. The current density−voltage (*J*−*V*) characteristics were measured on a computer−controlled Keithley 236 Source−Measure Unit. A xenon lamp coupled with AM 1.5 solar spectrum filter was used as the light source, and the optical power at the sample was 100 mW/cm^2.

Supporting Information Available: TGA and DSC plots, X-ray diffraction patterns and the OFET performance of the polymers. This information is available free of charge via the Internet at http://pubs.acs.org/.

Acknowledgements This work was supported by NSFC (#51103164, 50933003 and 21021091), The Ministry of Science and Technology of China (No: 2011AA050523 and 2010DFB63530) and Chinese Academy of Sciences (No. KGCX2-YW-399+9-1 and GJHZ1124).

References

[1] Yu, G.; Gao, J.; Hummelen, J. C.; Wudl, F.; Heeger, A. J. *Science*. **1995**, *270*, 1789.

[2] (a) Li, Y. F. *Acc. Chem. Res*. **2012**, *45*, 723. (b) Li, Y. F. Zou, Y. P. *Adv. Mater*. **2008**, *20*, 2952.

[3] Chen, J. W.; Cao, Y. *Acc. Chem. Res*. **2009**, *42*, 1709.

[4] (a) Cheng, Y.-J.; Yang, S.-H.; Hsu, C.-S. *Chem. Rev*. **2009**, *109*, 5868. (b) Chang, C.-Y.; Cheng, Y.-J.; Hung, S.-H.; Wu, J.-S.; Kao, W.-S.; Lee, C.-H.; Hsu, C.-S. *Adv. Mater*. **2012**, *24*, 549.

[5] (a) Chen, H.-Y.; Hou, J. H.; Zhang, S. Q.; Liang, Y. Y.; Yang, G. W.; Yang, Y.; Yu, L. P.; Wu, Y.; Li, G. *Nature Photonics*, **2009**, *3*, 649. (b) Huo, L. J.; Zhang, S. Q.; Guo, X.; Xu, F.; Li, Y. F.; Hou, J. H. *Angew. Chem. Int. Ed*. **2011**, *50*, 9697.

[6] (a) Liang, Y.; Yu, L. *Acc. Chem. Res*. **2010**, *43*, 1227. (b) Liang, Y.; Xu, Z.; Xia, J.; Tsai, S.-T.; Wu, Y.; Li, G.; Ray, C.; Yu, L. *Adv. Mater*. **2010**, *22*, E135.

[7] (a) Zhou, H.; Yang, L.; You, W. *Macromolecules*, **2012**, *45*, 607. (b) Chu, T.-Y.; Lu, J.; Beaupré, S.; Zhang, Y.; Pouliot, J.-R.; Wakim, S.; Zhou, J.; Leclerc, M.; Li, Z.; Ding, J.; Tao, Y. *J. Am. Chem. Soc*. **2011**, *133*, 4250. (c) Piliego, C.; Holcombe, T. W.; Douglas, J. D.; Woo, C. H.; Beaujuge, P. M.; Fréchet, J. M. J. *J. Am. Chem. Soc*. **2010**, *132*, 7595. (d) Bijleveld, J. C.; Zoombelt, A. P.; Mathijssen, S. G. J.; Wienk, M. M.; Turbiez, M.; Leeuw, D. M. de; Janssen, R. A. J. *J. Am. Chem. Soc*. **2009**, *131*, 16616. (e) Zhou, N.; Guo, X.; Ortiz, R. P.; Li, S.; Zhang, S.; Chang, R. P. H.; Facchetti, A.; Marks, T. J. *Adv. Mater*. **2012**, *24,* 2242. (f) Ong, K.-H.; Lim, S.-L.; Tan, H.-S.; Wong, H.-K.; Li, J.; Ma, Z.; Moh, L. C. H.; Lim, S.-H.; de Mello, J. C.; Chen, Z.-K. *Adv. Mater*. **2011**, *23*, 1409. (e) Qin, R.; Li, W.; Li, C.; Du, C.; Veit, C.; Schleiermacher, H.-F.; Andersson, M.; Bo, Z.; Liu, Z.; Inganas, O.; Wuerfel, U.; Zhang, F. *J. Am. Chem. Soc*. **2009**, *131*, 14612. (g)Wang, E.; Hou, L.; Wang, Z.; Hellström, S.; Zhang, F.; Inganäs, O.; Andersson, M. R. *Adv. Mater*. **2010**, *22*, 5240.

[8] (a) Jiang, J.-M.; Yang, P.-A.; Chen, H.-C.; Wei, K.-H. *Chem. Commun*. **2011**, *47*, 8877–8879. (b) Yuan, M.-C.; Chiu, M.-Y.; Liu, S.-P. Chen, C.-M.; Wei, K.-H. *Macromolecules*. **2010**, *43*, 6936. (c) Su, M.-S.; Kuo, C.-Y.; Yuan, M.-C.; Jeng, U. S.; Su, C.-J.; Wei, K.-H. *Adv.*

Mater. **2011**, *23*, 3315. (d) Chen, Y.-C.; Yu, C.-Y.; Fan, Y.-L.; Hung, L.-I.; Chen, C.-P.; Ting, C. *Chem. Commun*. **2010**, *46*, 6503.

[9] (a) Ahmed, E.; Subramaniyan, S.; Kim, F. S.; Xin, H.; Jenekhe, S. A. *Macromolecules*, **2011**, *44*, 7207. (b) Schroeder, B. C.; Huang, Z.; Ashraf, R. S.; Smith, J.; D'Angelo, P.; Watkins, S. E.; Anthopoulos, T. D.; Durrant, J. R.; McCulloch, I. *Adv. Funct. Mater*. **2012**, 22, 1663.(c) Zhou, E.; Yamakawa, S.; Tajima, K.; Yang, C.; Hashimoto, K. *Chem. Mater*. **2009**, *21*, 4055. (d) Zou, Y.; Najari, A.; Berrouard, P.; Beaupré, S.; Réda Aich, B.; Tao, Y.; Leclerc, M. *J. Am. Chem. Soc*. **2010**, *132*, 5330.(e) Li, Z.; Ding, J.; Song, N.; Lu, J.; Tao, Y. *J. Am. Chem. Soc*. **2010**, *132*, 13160. (f) Shi, Q.; Fan, H.; Liu, Y.; Hu, W.; Li, Y.; Zhan, X. *Macromolecules* **2011**, *44*, 9173.

[10] He, Y. J.; Li, Y. F; *Phys. Chem. Chem. Phys*. **2011**, *13*, 1970.

[11] (a) Hou, J. H.; Tan, Z. A.; Yan, Y.; He, Y. J.; Yang, C. H.; Li, Y. F. *J. Am. Chem. Soc*. **2006**, *128*, 4911. (b) Hou, J. H.; Huo, L. J.; He, C.; Yang, C. H.; Li, Y. F. *Macromolecules*. **2006**, *39*, 594. (c) Zhou, E. J.; Tan, Z. A.; Huo, L. J.; He, Y. J.; Yang, C. H.; Li, Y. F. ***J. Phys. Chem. B***., **2006**, *110*, 26062.

[12] Zou, Y. P.; Wu, W. P.; Sang, G. Y.; Yang, Y.; Liu, Y. Q.; Li, Y. F.; *Macromolecules*. **2007**, *40*, 7231.

[13] (a) Zhang, Z.-G.; Zhang, S.; Min, J.; Cui, C.; Zhang, J.; Zhang, M.; Li, Y.; *Macromolecules*. **2012**, *45*, 113. (b) Zhang, Z.-G.; Zhang, S. Y.; Min, J.; Cui, C. H.; Geng, H.; Shuai, Z. G.; Li, Y. F. *Macromolecules*. **2012**, *45*, 2312.

[14] Zhang, Z.-G.; Wang, J. Z.; *J. Mater. Chem*. **2012**, *22*, 4178.

[15] Huang, F.; Chen, K.-S.; Yip, H.-L.; Hau, S. K.; Acton, O.; Zhang, Y.; Luo, J.; Jen, A. K. Y. *J. Am. Chem. Soc*. **2009**, *131*, 13886.

[16] (a) Zhang, Z.-G.; Liu, Y.-L.; Yang, Y.; Hou, K.; Peng, B.; Zhao, G.; Zhang, M.; Guo, X.; Kang, E.-T.; Li, Y. F. *Macromolecules*. **2010**, *43*, 9376. (b) Zhang, Z.-G. Fan, H.; Min, J.; Zhang, S.; Zhang, J.; Zhang, M.; Guo, X.; Zhan, X.; Li, Y. F. *Polym. Chem*. **2011**, *2*, 1678.

[17] (a) Zhang, Z. H.; Peng, B.; Liu, B.; Pan, C. Y.; Li, Y. F.; He, Y. H.; Zhou, K. C.; Zou, Y. P. *Polym. Chem*. **2010**, *1*, 1441. (b) Min, J.; Zhang, Z.-G.; Zhang, S. Y.; Zhang, M. J.; Zhang, J.; Li, Y.F. *Macromolecules.* **2011**, *44*, 7632.

[18] Price, S. C.; Stuart, A. C.; Yang, L.; Zhou, H.; You, W. *J. Am. Chem. Soc*. **2011**, *133*, 4625.

[19] Zhou, H.; Yang, L.; Stuart, A. C.; Price, S. C.; Liu, S.; You, W.; *Angew. Chem. Int. Ed*. **2011**, *50*, 2995.

[20] Huo, L. J.; Hou, J. H.; Zhang, S. Q.; Chen, H.-Y.; Yang, Y. *Angew. Chem. Int. Ed*. **2010**, *49*, 1500.

[21] (a) Wang, M.; Hu, W.; Liu, P.; Li, W.; Gong, X.; Huang, F.; Cao, Y. *J. Am. Chem. Soc*. **2011**, *133*, 9638. (b) Peng, Q.; Liu, X.; Su, D.; Fu, G.; Xu, J.; Dai, L. *Adv. Mater*. **2011**, *23*, 4554.

[22] Ma, W.; Yang, C.; Gong, X.; Lee, K.; Heeger, A. J. *Adv. Funct. Mater*. **2005**, *15*, 1617

[23] Sun, Q.; Wang, H.; Yang, C.; Li, Y. F. *J. Mater. Chem*. **2003**, *13*, 800.

[24] Huo, L. J.; Guo, X.; Zhang, S. Q.; Li, Y. F.; Hou, J. H. *Macromolecules.* **2011**, *44*, 4035.

For “Table of Content” use only

Title: Conjugated Sidechain Isolated D-A Copolymers Based on Benzo[1,2-b:4,5-b']dithiophene-alt-dithienylbenzotriazole: Synthesis and Photovoltaic Properties

Authors: Jie Min, Zhi-Guo Zhang*, Siyuan Zhang, and Yongfang Li*